Thermodynamic and Kinetic Effects in the Aggregation Behavior of a Poly(ethylene glycol-*b*-propylene sulfide-*b*-ethylene glycol) *ABA* Triblock Copolymer

Simona Cerritelli,[†] Antonella Fontana,[‡] Diana Velluto,[‡] Marc Adrian,[§] Jacques Dubochet,[§] Paolo De Maria,[‡] and Jeffrey A. Hubbell*,[†]

Integrative Biosciences Institute, Ecole Polytechnique Fédérale de Lausanne (EPFL), Lausanne, Switzerland. Dipartimento di Scienze del Farmaco, Università "G. d'Annunzio", Chieti Italy, and Laboratoire d'Analyse Ultrastructurale, Université de Lausanne, Lausanne, Switzerland

Received June 6, 2005; Revised Manuscript Received July 12, 2005

ABSTRACT: We explore the effects of preparation protocol on the morphology and stability of aggregates from a poly(ethylene glycol-*b*-propylene sulfide-*b*-ethylene glycol) triblock copolymer, $PEG_{44}-PPS_{76}-PEG_{44}$. Fluorescence spectra and excimer formation of the probe molecule pyrene elucidated the various stages of aggregate formation, and cryo-TEM yielded insight into aggregate morphology. When prepared by direct hydration of polymer films, an extraordinary variety of morphologies was formed, ranging from spherical micelles to wormlike micelles, Y-junctions, blackberry micelles, and vesicles. Aging produced more uniform structural ensembles, including wormlike micelles with undulations and eventually spherical micelles, indicating the nonequilibrium nature of the system as initially formed. On the contrary, preparation by dilution from organic solvent yielded only structures that were closer to equilibrium distributions.

Introduction

The dual character of amphiphilic block copolymers leads to their self-assembly when dispersed in solvents that selectively solubilize only one of their domains. The driving force for aggregation in water is the tendency of a hydrophobic domain to minimize its contact with water and for the hydrophilic chains to orient themselves toward the aqueous phase and become solvated. In dilute systems, a variety of discrete aggregates can be formed.[1−3] It has been demonstrated that block copolymers can form classical aggregates such as spherical micelles, wormlike micelles[4,5] and vesicles,[6] similar to conventional low molecular weight amphiphiles and natural phospholipids. However, polymeric amphiphiles can also create a wide range of other morphologies that are not possible with natural phospholipids. Jain and Bates[1] described the appearance of Y-junctions, three-dimensional networks, spherical caps, and cylindrical loops for a poly(1,2-butadiene-*b*-ethylene glycol) (PBD-PEG) diblock copolymer above a critical molecular weight. The same authors depicted wormlike micelles, short cylinders with undulations, and octopus-like micelles using cryo-transmission electron microscopy (cryo-TEM).[7] The morphology of a block copolymer aggregate results from a balance of three different contributions: condensation of the hydrophobic chain, interfacial energy, and repulsion between hydrophilic groups.[4,5] Therefore, morphological variations can be induced by altering block copolymer composition and concentration,[3,5] changes in temperature, addition of ions[8,9] or organic solvents,[5] and modification in the protocols for preparation.

An important aspect of classical surfactant micelles is the dynamic exchange of monomers between micelles and the bulk solution.[10] This exchange occurs for surfactant molecules within microseconds.[10] The dynamics of block copolymer chain exchange among micelles and bulk solution has also been studied,[5,11−13] and the mobility of block copolymers has been found to be very different from that of low molecular weight surfactants. In particular, when the dispersing liquid is a very poor solvent for the hydrophobic domain, the mobility of the micellar core may be so low that it can be considered to be totally frozen.[11] Therefore, although the morphologies of aggregates of classical amphiphiles are mainly controlled by thermodynamics, kinetic effects can determine the formation of an extraordinary variety of metastable aggregates in the case of polymeric amphiphiles.

Polymeric aggregates can be obtained from selected polymer systems by diluting a copolymer dissolved in a good solvent for both blocks into water, a selective solvent for one block. The loss of solvent into the bulk aqueous solution drives the aggregation of the hydrophobic blocks.[3,5,8,9,14] In the hydrophobic core of the aggregates, perhaps still swollen by the organic solvent,[5] the polymer chains reorganize to gain a minimum interfacial tension. Despite reorganization within an aggregate, the presence of water surrounding each aggregate can dramatically slow the exchange of the polymer chains between the aggregates and the bulk solution.

Aggregates can also be formed from selected polymer systems by direct hydration of thin films in water. However, this method only works when using shorter, amorphous polymers above their T_g.[1] In this case, both intra- and interaggregate exchange of the polymer chains are low, reorganization within the aggregate being limited by chain entanglement, for example. Thus,

* To whom correspondence should be addressed. Address: Integrative Biosciences Institute, Ecole Polytechnique Fédérale de Lausanne (EPFL), LMRP Station 15, CH-1015 Lausanne, Switzerland. Tel: +41 21 693 9681. Fax: +41 21 693 9665. E-mail: jeffrey.hubbell@epfl.ch.

[†] Ecole Polytechnique Fédérale de Lausanne.

[‡] Università "G. d'Annunzio".

[§] Université de Lausanne.

10.1021/ma051176u CCC: $30.25
Published on Web 08/13/2005

these aggregates are more kinetically frozen in their initial structure, giving rise to the formation of complex metastable assemblies.

This study deals with the aggregation behavior of poly(ethylene glycol-*b*-propylene sulfide-*b*-ethylene glycol) (PEG−PPS−PEG), a triblock copolymer formed by two hydrophilic poly(ethylene glycol) (PEG) chains flanking a central hydrophobic poly(propylene sulfide) (PPS) chain. The PEG−PPS−PEG system is analogous to the well-characterized[15] poly(ethylene glycol-*b*-propylene glycol-*b*-ethylene glycol) system (referred to as Pluronics or Poloxamers); however, the substitution of the oxygen atom in the chain backbone of poly(propylene glycol) with the sulfur atom of PPS renders the central block considerably more hydrophobic. We are interested in PEG−PPS−PEG both from a fundamental perspective as well as for possible applications in drug delivery; the central block can be oxidized under relatively mild conditions, yielding the hydrophilic poly(propylene sulfone), allowing a novel mechanism of aggregate destabilization and potentially drug release.[18,19]

The fluidity of the hydrophobic domain of PEG−PPS−PEG, with PPS having a T_g of −60 °C,[16] confers at least some level of intrinsic mobility to the hydrophobic core at temperature of use. Here we explore the dependence of both the aggregate morphology and stability upon sample preparation protocol. In one protocol, hypothesized to yield structures closer to their equilibrium nature, a solution of copolymer in THF (a solvent for both blocks) is diluted in a very large volume of buffered saline (a nonsolvent for the PPS block). In a second, hypothesized to yield structures far from equilibrium, a thin copolymer film is hydrated and extruded through a nanoporous membrane. We apply fluorescence probe techniques and cryo-TEM to explore the structures that can be formed by these macroamphiphiles and their thermodynamically stable vs metastable character and exploit this knowledge in designing new drug delivery systems.

Materials and Methods

Poly(ethylene glycol-*b*-propylene sulfide-*b*-ethylene glycol), with degree of polymerization of 44 on the PEG and 76 on the PPS (abbreviated as $PEG_{44}-PPS_{76}-PEG_{44}$) was synthesized as reported elsewhere.[17] The molecular weight distribution was determined by size-exclusion chromatography (SEC) on a Polymer Laboratories column in THF. The M_n data were obtained using a universal calibration with PEG standards. The M_w/M_n of the polymer is 1.22. The molecular weight of the PPS domain was then confirmed from ^{1}H NMR measurements. The value was in agreement with that obtained from SEC data by subtraction of the PEG molecular weight, taken as declared from the vendor.

All solvents and reagents were purchased from Fluka or Aldrich and used without further purification.

Sample Preparation. In one sample preparation protocol, a copolymer stock solution was prepared in THF, at 1 wt % copolymer, and a given volume was diluted in 2 mL of phosphate-buffered saline (PBS, 137 mM NaCl, 3 mM KCl, 10 mM Na_2HPO_4, in double-distilled water, pH 7.4) to obtain the desired final polymer concentration. In a second protocol, 10 mg of copolymer were dissolved in 1 mL of THF and were slowly dried by rotary evaporation. The flask was kept under reduced pressure for 12 h to remove the organic solvent and to obtain a thin homogeneous polymer film. This film was then exposed to 1 mL of PBS under vigorous stirring. The aggregates formed by this procedure were passed through a nanoporous polycarbonate filter (200 nm pores, Osmonic) several times using a liposome extruder (Lipex thermo barrel extruder, Northern Lipids). All sample preparation was done at room temperature.

Fluorescence Measurements. Fluorescence probe techniques, using pyrene, were used to evaluate the critical micelle concentration of the copolymer and to characterize the hydrophobic domains of the aggregates. Pyrene changes its fluorescence emission spectrum in response to the polarity of its environment and can be used to characterize the hydrophobic cores of such aggregates.[20] Using this well characterized probe,[21] an empirical "pyrene scale" has been catalogued for a wide variety of bulk liquids,[22] surfactant micelles, and interfacial monolayers.[23−25] The solvent polarity dependence of pyrene's emission is expressed in terms of the ratio I_1/I_3, which are the intensities of bands I and III corresponding to $S_1^{\nu=0} \rightarrow S_0^{\nu=0}$ (0−0) and $S_1^{\nu=0} \rightarrow S_0^{\nu=1}$ (0−1) transitions, respectively, S_1 and S_0 being first singlet excited state and ground state, respectively. The values collected over the years from different research groups[21,22,26] typically range from 1.2 to 2.0 in polar solvents to ≈0.6 in hydrocarbons. It is important to mention here that pyrene I_1/I_3 values obtained by different authors show some discrepancies due to the dependence of I_1/I_3 values on several experimental variables such as excitation wavelength, excitation/emission slit widths, self-adsorption due to pyrene concentration effects, inner-filtering artifacts, and temperature. Nevertheless, a polar solvent such as water shows always at a high value ranging between 1.59[21] and 1.87,[22] whereas apolar solvents show low I_1/I_3 values ranging between 0.55 and 0.60.[21,22] Despite such discrepancies, this technique remains fundamental for the determination, at a constant pyrene concentration, of the critical aggregation concentration of an amphiphile, obtained as the amphiphile concentration at which I_1/I_3 sharply decreases, reflecting the preferential solubilization of pyrene in a hydrophobic environment.

Pyrene also forms excimers, when an electronically excited pyrene molecule encounters a second pyrene molecule in its ground electronic state.[27] Accordingly, the two pyrene molecules must be far from each other when light is absorbed, so only one of them is excited, but mobile, so as to be able to encounter each other. From our static fluorescence experiments, it is not possible to distinguish whether the emission is due to such "dynamic" excimers or to the so-called "static excimers" that are obtained from ground-state pyrene dimers.[28] Regardless, in both cases the dimer can only be obtained through encounter of two molecules and thus depends on the microviscosity of the aggregates and in turn their organization and packing.[29,30] Therefore, the ratio of the fluorescence intensity of the excimer to monomer (I_E/I_M) provides information on the distribution of the probe molecules in the aggregate and on the microviscosity of the system, a high ratio corresponding to a low microviscosity.[31]

Steady-state fluorescence spectra were recorded at 25 °C using a Jasco FP662 spectrofluorometer with a band-pass of 5 nm. A given volume of a pyrene (98%, Aldrich) stock solution in ethanol (2×10^{-3} M) was added to the aggregate suspension under stirring and left to equilibrate for at least 3 min before performing the measurement. The excitation wavelength was chosen at $\lambda_{ex} = 335$ nm as no significant difference in the excitation spectra was found between the λ_{ex} of pyrene in water and that in the aggregate.[32] The monomer emission was read at $\lambda_{em} = 377$ (I_1) and $\lambda_{em} = 386$ (I_3), whereas the excimer emission was read at $\lambda_{em} = 480$ nm. Preliminary tests were performed to evaluate, at a fixed polymer concentration of 1×10^{-5} M, the concentrations of pyrene at which the emissions of the excimer is completely absent or better it is well detectable (it reaches a values that can be considered a good compromise between excimer detection and the need to keep as low as possible the ratio [pyrene]/[polymer]). In this way, two concentrations of pyrene were chosen: 2×10^{-6} M to study the monomer emission (and to determine the corresponding I_1/I_3) and 5×10^{-5} M to study the emission of the excimer (and to determine the corresponding I_E/I_M).

Cryo-Trasmission Electron Microscopy. Cryo-TEM[33] was used to investigate the morphology of the $PEG_{44}-$

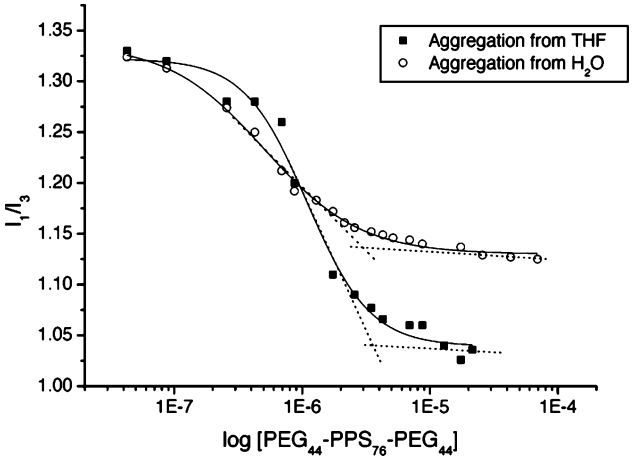

Figure 1. Plot of the fluorescence intensity ratio I_1/I_3 as a function of $PEG_{44}-PPS_{76}-PEG_{44}$ concentration. The samples were prepared by dilution of a polymer solution in THF into buffered saline (filled squares) or by direct hydration of thin copolymer films in buffered saline (open circles). Pyrene concentration was kept constant at 2×10^{-6} M. A critical micelle concentration of about 3×10^{-6} M has been measured for both series. The results indicate the presence of pre-micelles at very low concentration and of micelles at higher polymer concentration. Micelles formed by dilution from THF are less polar in their cores than those formed by direct hydration.

$PPS_{76}-PEG_{44}$ aggregates prepared by both protocols described above. For measurement from THF, a few microliters of a stock solution in THF of 10 wt % copolymer was diluted in PBS to give a final copolymer concentration of 0.5 or 1 wt %. For measurements directly in PBS, the already described procedure of preparation of the samples has been followed, with the final concentration of 1 wt % copolymer. The specimens for analysis were prepared by application of a drop of the aqueous aggregate suspension on a micro copper grid coated with a porous carbon film. Excess suspension was blotted away, resulting in a 30−100 nm thick film that spans the holes of the porous carbon support. The sample was then rapidly vitrified by immersion in liquid ethane, transferred to the cryo-electron microscope Philips CM12 (FEI, Eindhoven, The Netherland) operating at 100 kV in transmission mode at a temperature never exceeding −160 °C. Images were recorded on CCD camera with minimum electron dose at a nominal magnification of up to 45000×. Unless otherwise specified, images were acquired within 24 h of preparation of the aggregate suspension.

Results and Discussion

Probe Analyses: Aggregation from THF Solutions. One aggregate preparation protocol involved dissolving $PEG_{44}-PPS_{76}-PEG_{44}$ in THF and diluting this solution in a large volume of water. When this copolymer solution is diluted in the selective solvent water, the hydrophobic effect drives the PPS domain to aggregate, the PEG chains rearranging and stretching their coils around the hydrophobic PPS core. A critical micellar concentration of about 3×10^{-6} M could be measured, both in water (data not shown) and in PBS, by means of the above-mentioned pyrene method.[20,21,28]

I_1/I_3 values were collected at different polymer concentrations and constant pyrene concentration (see Figure 1, squares). As one considers this curve beginning from low polymer concentration, several features become apparent. First, even at the lowest polymer concentration studied, i.e., already at 5×10^{-8} M, 60 times lower than the critical micelle concentration, the initial measured I_1/I_3 is 1.30−1.35. Such a value is quite low, as I_1/I_3 for the same probe in bulk water ranges from 1.6[21] to 1.9.[22] Granted that a comparison with previous reported data is difficult, the onset of the decrease in I_1/I_3, at around 2×10^{-7} M implies that even under very dilute conditions, 15 times lower than the critical micelle concentration, the block copolymer has self-organized into pre-micellar aggregates bearing a hydrophobic region in which the pyrene solubilize.[35,36] Such pre-micellar aggregates have a higher micropolarity than proper micelles due to the different structure, micelles being much more organized, compact, and less polar objects. The gradual decline in the I_1/I_3 ratio covers the surfactant concentration range $2 \times 10^{-7}-3 \times 10^{-6}$ M. This large interval of concentrations during aggregation can be ascribed to the processes of growth of the aggregates, i.e., increase in their aggregation number.[28] Finally, at higher polymer concentrations, the I_1/I_3 ratio reaches a stable minimum of about 1.03. This plateau indicates that the aggregates have reached an optimum aggregation number forming true micelles in which the probe experiences an environment with a micropolarity considerably lower than that of the bulk aqueous phase. The obtained final I_1/I_3 value indicates that the micelles have a polarity similar to that of a primary alcohol such as 1-butanol ($I_1/I_3 = 1.02$[21]-1.06).[22] Similar values have been obtained previously for several micelles[21] and block copolymer aggregates.[34]

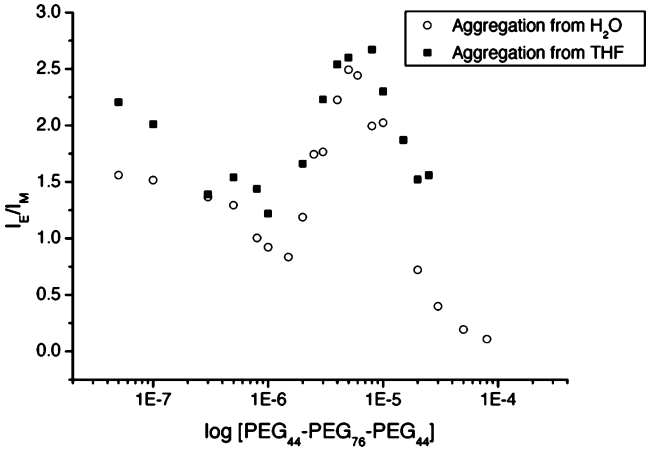

Figure 2. Plot of the fluorescence I_E/I_M ratio as a function of $PEG_{44}-PPS_{76}-PEG_{44}$ concentration. The samples were prepared by dilution of a polymer solution in THF into buffered saline (filled squares) or by direct hydration of thin copolymer films in buffered saline (open circles). Pyrene concentration was kept constant at 5×10^{-5} M. Both the pre-micellar aggregates (at low copolymer concentration) and the micelles (at high copolymer concentration) formed by dilution from THF are more fluid than those formed by direct hydration.

Further characterization of the aggregates could be obtained from study of the probe excimer formation in the presence of different polymer concentrations. The plot of I_E/I_M for the $PEG_{44}-PPS_{76}-PEG_{44}$ suspension in the presence of 5×10^{-5} M pyrene is depicted in Figure 2 (squares). The results are typical for amphiphilic polymers that aggregate in water. An initial decrease of the excimer-to-monomer emission ratio with increasing copolymer concentration was observed, reaching a minimum at a polymer concentration of 1×10^{-6} M. This behavior confirms the formation, as mentioned above, of small pre-micellar aggregates in which the pyrene molecules can preferentially solubilize. As the polymer concentration is increased, the number of these aggregates increases, and the probability of multiple pyrene molecules sharing the same aggregate is lowered, leading to the decreasing I_E/I_M ratio. At polymer

concentrations higher than 1×10^{-6} M the I_E/I_M ratio increases with increasing polymer concentration, up to a maximum. This clearly indicates the formation of larger and more fluid multimolecular aggregates in which the chance of having more than one pyrene molecule per aggregate, and the probability of excimers formation, is higher. The maximum value of I_E/I_M is observed at a polymer concentration of 6×10^{-6} M, close to the critical micelle concentration found using the I_1/I_3 method (3×10^{-6} M). Upon further increase in polymer concentration, the dilution effect by increasing the number of micelles at constant pyrene concentration plays a dominant role and results in decreasing I_E/I_M.[37,38]

Probe Analyses: Aggregation from Rehydration in PBS and Comparison of the Two Protocols. A second aggregation protocol was explored, in which thin $PEG_{44}-PPS_{76}-PEG_{44}$ copolymer films were directly hydrated with PBS. It is well-known that different preparation protocols affect the aggregation behavior of block copolymers due to the specific kinetics of the aggregation process associated with the hydrophobic chains, the mobility of the corona-forming chains,[5,8] and the low monomer-aggregate and aggregate-solvent interactions. We were interested to know if the two methods, i.e., dilution from solvent into a selective solvent and direct hydration, differed in the closeness to equilibrium of the formed structures. As with the first protocol, both I_1/I_3 and I_E/I_M ratios were measured.

The data obtained from the monomer emissions are reported in Figure 1 as open circles. The profile of I_1/I_3 vs polymer concentration is qualitatively similar to that observed for dilution from solvent: at low polymer concentration (already at 5×10^{-8} M, 60 times lower than the critical micelle concentration), pre-micellar aggregates were formed, and at higher polymer concentration, micelles were observed. Likewise, the profile of I_E/I_M was qualitatively similar, reported in Figure 2 as open circles: excimer formation was observed in the pre-micellar aggregates, and somewhat easier excimer formation was observed with respect to the micelles formed at higher concentration, indicative of higher micro-fluidity.

Quantitative comparison of I_1/I_3 and I_E/I_M of samples prepared by the two preparation protocols suggests the presence of distinct morphological characteristics. Considering first the structures formed at low polymer concentration, the polar character of the pre-micelles did not seem to depend on preparation method (refer to I_1/I_3 at the onset of decrease), whereas the structures formed by dilution from THF appear to be more fluid than those from direct hydration (as judged from I_E/I_M). This evidence points out that intermediate morphologies are not simply rationalizable as a consequence of hydrating sheets of dry copolymer which then break up via complex mechanisms. If this was the case, only the hydration protocol would have favored their formation according to the lamellar phase formed upon hydration of the dry copolymer.[17,39] At higher polymer concentration, where proper micelles are observed, the polarity of the micelles formed by dilution from THF is much lower than that in micelles formed from direct hydration (refer to I_1/I_3), and moreover these micelles are much more fluid (refer to I_E/I_M). It could be that the micelles formed by THF dilution retain a small amount of THF in their hydrophobic cores, yielding the lower polarity and higher fluidity. In any case, it is safe to make the first conclusion that the micelles obtained from THF harbor an environment in their cores that is less polar and more fluid than in micelles obtained by direct hydration.[41] Nevertheless, independently of the preparation protocol, the micellar core of the investigated $PEG_{44}-PPS_{76}-PEG_{44}$ copolymer appears to be more hydrophobic than the micellar core of analogous Pluronics ($I_1/I_3 > 1.4$),[42] in agreement with the substitution of the sulfur atom of PPS with the oxygen atom of PPO. Second, the results in the I_1/I_3 trace indicate the formation of pre-micellar aggregates at lower concentration by direct hydration than by dilution from THF (refer to the earlier decrease in I_1/I_3 as polymer concentration is increased). Thus, the molecular association transition for the directly hydrated polymer is quite broad, spanning almost 100-fold in polymer concentration, compared to the same process for the polymer diluted from THF. Since pyrene association with the micellar phase is strongly influenced by the size of the aggregates[40] these data indicate that the aggregates formed by using the two preparation protocols are very different in size, direct hydration leading to larger pre-micellar aggregates at moderate concentration. Last but not least, the different I_E/I_M values obtained for the two preparation protocols at low polymer concentrations indicates that the initial fluorescence is mostly due to dynamic, sensitive to the different fluidity of the systems, rather than static excimers.

Cryo-TEM Analyses. Consistent with results obtained by spectroscopic observation of the pyrene probe, aggregate structures formed by direct hydration of $PEG_{44}-PPS_{76}-PEG_{44}$ films were much larger and more complex.

Figure 3, panels a–d, reveals the coexistence of several morphologies of copolymer aggregates in samples prepared by direct hydration: spherical and wormlike micelles (Figure 3a,b), vesicles and vesicles containing micelles (Figure 3a,b,d), Y-junctions (Figure 3c,d) with no caps and Y-junctions with spherical caps which give raise to differently shaped multi-looped structures (blackberry micelles, Figure 3d) and eventually networks (Figure 3d).

The coexistence of complex morphologies for a single block copolymer has already been investigated in a similar system, as a function of the PEG composition.[43] A 1% colloidal suspension of poly(ethylene glycol-*b*-ethyl ethylene-*b*-ethylene glycol) (PEG–PEE–PEG) with a volume fraction of PEG (f_{EG}) = 0.44 revealed the formation of wormlike micelles, characterized by loops and branches, blackberry micelles, spherical, micelles, vesicles, and flat bilayer fragments. Increasing the PEG composition from 0.44 to 0.53 resulted in a pronounced micelle shortening and the disappearance of bilayers, as anticipated by molecular-packing considerations.[44] In a similar study[1] on two sets of poly(butadiene-*b*-ethylene glycol) (PB–PEG) diblock copolymers, it has been highlighted that, together with the hydrophilic domain, the dimensions of the hydrophobic domain have an important role in the structural determination of the corresponding aggregates. Increasing the size of the hydrophobic blocks shifts the composition window for wormlike micelles to lower values of f_{EG} and induces the formation of Y-junctions, cylindrical loops and spherical caps. It is noteworthy that our block copolymer with a $M_{w(PPS)}$ = 5600 g/mol (total molecular weight of only 9600 g/mol) and $f = 0.42$ forms loops and Y-junction as well as the much heavier PB–PEG copolymer, with

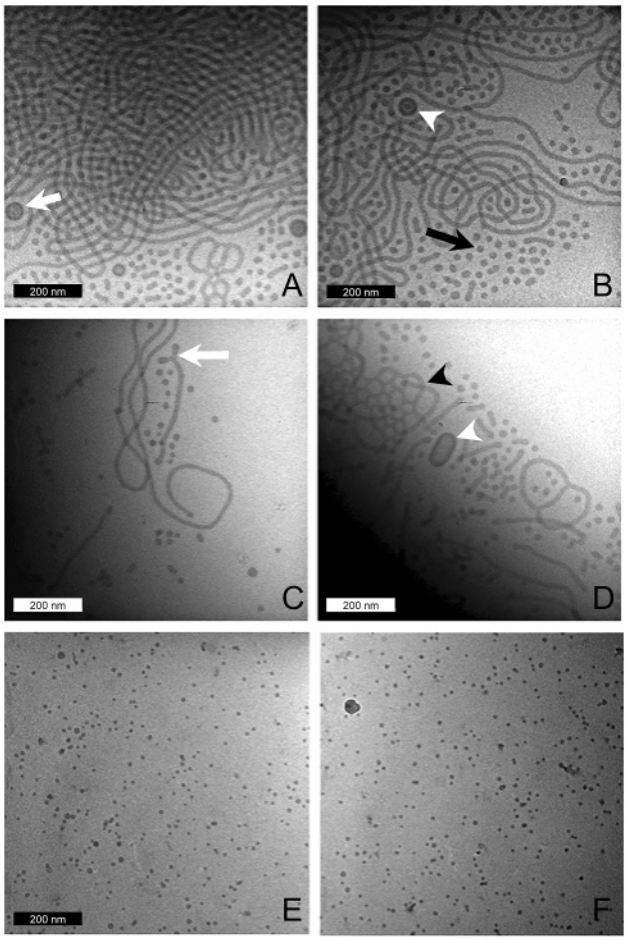

Figure 3. Cryo-TEM micrographs obtained from 0.5 or 1 wt % aqueous solution of PEG_{44}−PPS_{76}−PEG_{44}. In panels a−d, samples were prepared by direct hydration of copolymer films, and in panels e and f, samples were prepared by dilution from THF into buffered saline. (a−d) In the samples prepared by direct hydration, it is possible to see coexistence of a vast array of different aggregates: a preponderance of spherical micelles (black arrow) and long wormlike micelles (unmarked, but visible in a−d), as well as Y-junctions (white arrow) and blackberry micelles (black arrowhead). A few vesicles are also present (short white arrow), including one with a micelle inside (white arrowhead). (e, f) In the samples prepared by dilution of a polymer solution from THF into buffered saline, only spherical micelles were observed, which showed some degree of polydispersity.

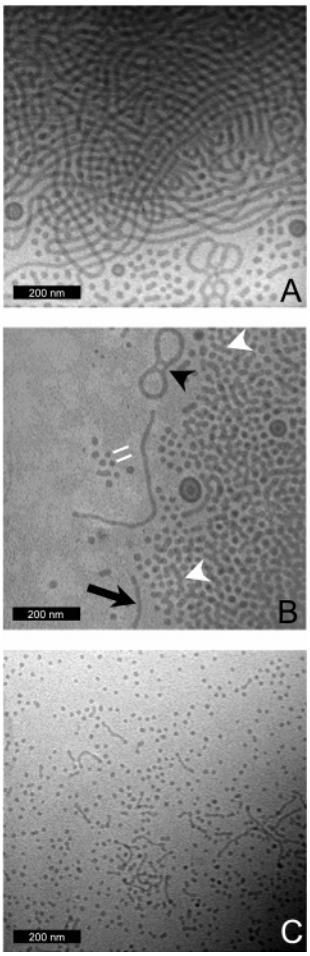

Figure 4. Cryo-TEM micrographs obtained from 0.5 or 1 wt % aqueous solution of PEG_{44}−PPS_{76}−PEG_{44} aged prior to imaging. In the total time span of 6 months it is possible to see simplification in the aggregate morphologies, approaching spherical micelles. (a) The sample imaged 24 h after formation shows the morphological complexity also reported in Figure 3, panels a−d. (b) After aging for 2 weeks, the majority of the cylindrical micelles have been transformed into much shorter worms (black arrows) and spherical micelles; only few looped structures still persist in the sample (black arrowhead). Notably, a number of very short worms exist with multiple undulations (white arrowheads). Note that in images of spherical micelles, the PEG corona forces a separation between the electron-dense PPS cores of spherical micelles (pair of white lines), and this separation is not present here in many of the electron dense undulations; this striking difference in spacing supports that these electron-dense globules are indeed undulations in the wormlike micelles, which we hypothesize to be in the process of transformation to spherical micelles. (c) After aging for 6 months, mostly spherical micelles can be observed, in addition to a smaller number of very short worms with undulations. The samples were aged at room temperature.

$M_{w(PB)}$ = 9200 g/mol and f_{EG} = 0.34.[1] As cited by Jain and Bates,[7] a possible explanation for the appearance of such branches even at a relatively low MW could be attributed to the effect of the polydispersity of the polymer. We address this point further below.

By stark contrast with the cryo-TEM results obtained by direct hydration, dilution from the good solvent THF yielded exclusively spherical micelles (Figure 3, panels e and f). In samples obtained from exactly the same polymer stock (i.e., same molecular weight, same polydispersity, etc.), the differences in aggregate structures are striking. No vesicles or wormlike micelles were observed, only spherical micelles.

The striking difference between morphologies obtained by the two protocols leads one to question to what extent the samples obtained by direct hydration represent equilibrium structures. Are the striking differences between Figure 3, panels a−d and e and f, due to the small amount of residual THF within the sample after dilution in the large volume of PBS upon preparation, or do the structures in Figure 3e,f represent a closer-to-equilibrium state, as hypothesized? To probe this, we aged a sample prepared by direct hydration: Figure 4 shows such a sample after 24 h, 2 weeks, and 6 months. Shortly after preparation, the dominant morphology in the sample was wormlike micelles, with spherical micelles, vesicles, and closed, multi-loop networks also being visible, a complex collection of diverse morphologies. After aging for 2 weeks, most of the wormlike micelles had disappeared, although some could be observed in addition to vesicles, loops, and, strikingly, very short worms with undulations. In the TEM images, the PPS core is visualized, and the PEG corona, which

is not visualized in the images, leads to a separation of the electron dense regions, for example spacing wormlike and spherical micelles by a more-or-less constant intervals. This separation is distinctly absent in many of the electron-dense globular regions of Figure 4b, leading us to conclude that these connected globular structures are undulations in metastable wormlike micelles that will eventually separate and become spherical micelles. This speculation may indeed be correct, as visualization of a sample after 6 months aging yielded a higher fraction of spherical micelles, with a smaller number of short worms with undulations still remaining. Interestingly, the spherical micelles obtained by aging appear very similarly to those obtained by dilution from THF, suggesting that the small amount of residual THF in the latter does not influence phase morphology greatly.

In their structurally similar, although higher molecular weight, system, Jain and Bates[7] suggested the possibility that coexisting complex morphologies, leading to the appearance of structures such as branches even at relatively low MW could be attributed to the effect of the polydispersity of the polymer, with a sort of nanophase separation to different regions of the nanostructures. With our system, we believe this to be unlikely. First, the polydispersity in our copolymer sample is low, being only a value of 1.22. More importantly, polydispersity did not change in the samples prepared by direct hydration as they aged over time, when the observed complex, coexisting morphologies gave way to simpler, more homogeneous ones. Thus, we suggest that, in our samples prepared by direct hydration, the complex, coexisting structures observed are merely metastable states, slowly on their way to a more regular and simple equilibrium.

Conclusions

The triblock copolymer $PEG_{44}-PPS_{76}-PEG_{44}$ tends to aggregate in water, and the morphology of the formed aggregates depends strongly on the protocol of preparation. We hypothesized that samples prepared by dilution of the copolymer from a good solvent into a selective solvent would yield aggregate morphologies that are closer to equilibrium than those prepared by direct hydration of thin copolymer films. This hypothesis was supported. Aggregates obtained by dilution from THF were small, less polar, less viscous, and less densely packed than those obtained by direct hydration, as indicated by probe spectroscopic methods. Cryo-TEM of samples obtained by THF dilution revealed spherical micelles. By stark contrast, cryo-TEM of samples obtained by direct hydration showed aggregates of an extraordinary variety of morphologies ranging from spherical micelles to wormlike micelles, Y-junctions, blackberry micelles, and vesicles. Aging experiments showed these aggregates to be unstable, giving way to spherical micelles and short wormlike micelles with undulations. Based on the similarly of morphologies obtained by THF dilution and aging after direct hydration, we conclude that the highly complex morphologies observed with $PEG_{44}-PPS_{76}-PEG_{44}$ by direct hydration are metastable, and that the additional mobility of the PPS domains conferred due to the initial presence of organic solvent greatly accelerates the approach of the system to equilibrium. On the other hand, the limited mobility of the PPS domains in water without the initial presence of solvent favors formation of a variety of kinetically trapped, metastable morphologies which, nevertheless, slowly but spontaneously tend to revert to spherical micelles with time.

Acknowledgment. We thank MIUR for financial support (COFIN 2004: Protocol Number 2004035502).

References and Notes

(1) Jain, S.; Bates, F. S. *Science* **2003**, *300*, 460−464.
(2) Discher, B.; Won, Y.-Y.; Ege, D. E.; Lee, J. C.-M.; Bates, F. S.; Discher, D. E.; Hammer, D. A. *Science* **1999**, *284*, 1143−1146.
(3) Zhang, L.; Eisenberg, A. *Science* **1995**, *268*, 1728−1731.
(4) Halperin, A.; Tirrell, M. Lodge, T. P. *Adv. Polymer. Sci*. **1992**, *100*, 31−71.
(5) Zhang, L.; Eisenberg, A. *Macromolecules* **1999**, *32*, 2239−2249.
(6) Discher, D. E.; Eisenberg, A. *Science* **2002**, *297*, 967−973.
(7) Jain, S.; Bates, F. S. *Macromolecules* **2004**, *37*, 1511−1523.
(8) Zhang, L.; Yu, K.; Eisenberg, A. *Science* **1996**, *272*, 1777−1779.
(9) Zhang, L.; Eisemberg, A. *Macromolecules* **1996**, *29*, 8805−8815.
(10) Clint, J. H. *Surfactant Aggregation*; Blackie & Son Ltd: London, 1992; p 101.
(11) Tian, M.; Qin, A.; Ramireddy, C.; Webber, S. E.; Munk, P. *Langmuir* **1993**, *9*, 1741−1748.
(12) Procházka, K.; Bednáø, B.; Mukhtar, E.; Svoboda, P.; Trnená, J.; Almgren, M. *J. Phys. Chem*. **1991**, *95*, 4563−4568.
(13) Wang, Y.; Kausch, M.; Chun, M.; Quirk, R. P.; Mattice W. L. *Macromolecules* **1995**, *28*, 904−911.
(14) Zhang, L.; Shen, H.; Eisemberg, A. *Macromolecules* **1997**, *30*, 1001−1011.
(15) Alexandridis, P.; Hatton, T. A. *Colloids Surf. A* **1995**, *1*, 1−46.
(16) Nicol, E.; Nicolai, T.; Durand, D. *Macromolecules* **1999**, *32*, 7530−7536.
(17) Napoli, A.; Tirelli, N.; Kilcher, G.; Hubbell, J. A. *Macromolecules* **2001**, *34*, 8913−8917.
(18) Napoli, A.; Boerakker, M. J.; Tirelli, N.; Nolte, R. J. M.; Sommerdijk, N. A. J. M.; Hubbell, J. A. *Langmuir* **2004**, *20*, 3487−3491.
(19) Napoli, A.; Valentini, M.; Tirelli, N.; Muller, M.; Hubbell, J. A. *Nature Materials* **2004**, *3*, 183−189.
(20) Winnik, F. M.; Regismond, S. T. A. *Colloids Surf. A* **1996**, *118*, 1−39.
(21) Kalyanasundaram K.; Thomas J. *J. Am. Chem. Soc.* **1977**, *99*, 2039−2044.
(22) Dong, D. C.; Winnik, M. A. *J. Can. Chem*. **1984**, *62*, 2560−2565.
(23) Grieser, F.; Drummond, C. J. *J. Phys. Chem*. **1988**, *92*, 5580−5593.
(24) Zana, R. *Surfactants in Solution: New Methods of Investigation*; Zana, R., Ed.; M. Dekker: New York, 1987; Chapter 5.
(25) Mazères, S.; Lagane, B.; Welby, M.; Trégou, V.; Lopez, A. *Spectrochim. Acta Part A* **2001**, *57*, 2297−2311.
(26) Street, K. W., Jr.; Acree, W. E., Jr. *Analyst* **1986**, *111*, 1197−1201 and references therein.
(27) Birks, J. B. *Rep. Prog. Phys*. **1975**, *38*, 903−974.
(28) Winnik, F. M. *Chem. Rev.* **1993**, *93*, 587−614.
(29) Heldt, N.; Gauger, M.; Zhao, J.; Slack, G.; Pietryka, J. and Li, Y. *React. Funct. Polym*. **2001**, *48*, 181−191.
(30) Winnik, F. M.; Winnik, M. A.; Tazuke, S. *J. Phys. Chem.* **1987**, *91*, 594−597.
(31) Turro, N. J.; Lei, X.-G.; Ananthapadmanabhan, K. P.; Aronson, M. *Langmuir* **1995**, *11*, 2525−2533.
(32) Wilhem, M.; Zhao, C.-L.; Wang, Y.; Xu, R., Winnik, M. A.; Mura, J.-L.; Riess, G.; Croucher, M. D. *Macromolecules* **1991**, *24*, 1033−1040.
(33) Dubochet, J.; Adrian, M.; Chang, J.-J.; Homo, J.-C.; Lepault, J.; McDowall, A. W.; Schultz, P. *Q. Rev. Biophys.* **1988**, *21*, 129−228.
(34) Zhao, C.-L.; Winnik, A. M.; Riess, G.; Croucher, M. D. *Langmuir* **1990**, *6*, 514−516.
(35) Chu, B. *Langmuir* **1995**, *11*, 414−421.
(36) Mathias, J. H.; Rosen, M. J.; Davenport, L. *Langmuir* **2001**, *17*, 6148−6154.
(37) Kim, J.-H.; Domach, M.; Tilton, R. D. *Langmuir* **2000**, *16*, 10037−10043.

(38) Pandit, N.; Trygstad, T.; Croy, S.; Bohoroquez, M.; Koch, C. *J. Colloid Interface Sci.* **1999**, *222*, 213−220.
(39) Napoli, A.; Tirelli, N.; Wehrli, E.; Hubbell, J. A. *Langmuir* **2002**, *18*, 8324−8329.
(40) Wang, Y.; Winnik, M. A. *Langmuir* **1990**, *6*, 1437−1439.
(41) Kim, J.-H.; Domach, M.; Tilton, R. D. *Langmuir* **2000**, *16*, 10037−10043.
(42) Alexandridis, P.; Nivaggioli, T.; Hatton, T. A. *Langmuir* **1995**, *11*, 1468−1476.
(43) Won, Y.-Y.; Brannan, A. K.; Davis, H. T.; Bates, F. S. *J. Phys. Chem. B* **2002**, *106*, 3354−3364.
(44) Israelachvili, J. *Intermolecular and Surface Forces*, 2nd ed.; Academic Press: San Diego, CA, 1992.

MA051176U